Disposition Of PF-07321332 (Nirmatrelvir), an Orally Bioavailable Inhibitor of SARS-CoV2 Main Protease, across Animals and Humans

Heather Eng[1], Alyssa L. Dantonio[1], Eugene P. Kadar[1], R. Scott Obach[1], Li Di[1], Jian Lin[1], Nandini C. Patel[2], Britton Boras[3], Gregory S. Walker[1], Jonathan J. Novak[1], Emi Kimoto[1], Ravi Shankar Singh[2], and Amit S. Kalgutkar[2]

Affiliations:

[1]Pfizer Worldwide Research, Development & Medical; Groton, CT 06340, USA

[2]Pfizer Worldwide Research, Development & Medical; Cambridge, MA 02139, USA

[3]Pfizer Worldwide Research, Development & Medical; La Jolla, CA 92121, USA

Journal Title Drug Metabolism and Disposition

Supplemental Information

Abbreviations:

P_{app}, apparent permeability; MDCKII-LE, low efflux Madin-Darby canine kidney cells; HBSS, Hanks balanced salt solution; BCRP, breast cancer resistant protein; MDR1, multidrug resistant gene 1; LC-MS/MS, liquid chromatography tandem mass spectrometry; $f_{u,p}$, unbound fraction in plasma; HLM, human liver microsomes; $f_{u,mic}$, unbound fraction in human liver microsomes; BPR, blood to plasma ratio; R_b, blood to plasma partitioning; NADPH, β-nicotinamide adenine dinucleotide phosphate, reduced form; CYP, cytochrome P450; $t_{1/2}$, half-life; $CL_{int,app}$, apparent intrinsic clearance; $CL_{int,scaled}$, scaled intrinsic clearance; CL_{hep}, hepatic clearance; iv, intravenous; po, oral; MTBE, methyl-tert-butyl ether; AUC, area under the plasma concentration-time curve; CL_p, plasma clearance; Vd_{ss}, steady state distribution volume; F, oral bioavailability; F_a x F_g, fraction of the oral dose absorbed; Q, hepatic blood flow; CL_{blood}, blood clearance; DF, dilution factor; CL_{renal}, renal clearance; $CL_{biliary}$, biliary clearance; IC_{50}, half-maximal inhibitory concentration; k_{inact}, maximal rate of inactivation; K_I, inactivator concentration at k_{inact}; mRNA, messenger RNA; Ind_{max}, maximal fold induction; EC_{50}, inducer concentration that produces half Ind_{max}; HEK, human embryonic kidney cells; OAT, organic anion transporter; OCT, organic cation transporter; MATE, multidrug and toxin extrusion protein; OATP, organic anion transporting polypeptide.

Materials and Methods.

Passive Permeability Studies. Apparent permeability (P_{app}) of PF-07321332 was measured in Caco-2 (ATCC, Manassas, Manassas, VA) and in low efflux Madin-Darby canine kidney (MDCKII-LE) cell lines in triplicate with a modification to previously reported methodology (Di et al., 2011; Varma et al., 2012). For the MDCKII-LE assay, the modification included addition of 0.4% bovine serum albumin to the receiver compartment to minimize nonspecific binding, and thus maximize recovery of the analyte from the wells upon permeation across the cell monolayers. Briefly, MDCKII-LE cells were seeded onto the apical chambers of Millicell 96-well Transwell Plate (MilliporeSigma, Atlanta, GA) with 2.64×10^4 cells/well (0.1 ml of 2.64×10^5 cells/ml). Cells were incubated for 4 days at 37 °C, 5% CO_2, 90% relative humidity. On the assay day, PF-07321332 and control compounds (atenolol, nadolol, cyclosporin A, and metoprolol) were tested at 6 µM.

Caco-2 cells were seeded at 7.15 x 10^3 cells/well in 96-well transwell plates, and cultured in Dulbecco's modified eagle's medium-high glucose supplemented with 20% fetal bovine serum, 1% non-essential amino acids, 1% glutamax, 1% sodium pyruvate, and 0.6% gentamicin for 21 days. For donor solutions, final assay concentrations of PF-07321332 in the presence or absence of inhibitor cocktail were prepared using Hanks balanced transport buffer (HBSS) supplemented with 20 mM 4-(2-hydroxyethyl) piperazine-1-ethanesulfonic acid and 25 mM glucose). Receiver solutions contained 0.4% bovine serum albumin, with or without inhibitor cocktail. Inhibitor cocktail was made up of 10 µM Ko143 (BCRP inhibition), 10 µM PSC833 (MDR1 inhibition), and 100 µM MK571 (multi-drug resistance protein inhibition). Apical-to-basolateral (A-B) transport assay was started by the addition of donor and receiver solutions to the apical and basolateral compartments, respectively. The plates were then incubated for 1.5 hours at 37 °C. The transport assay was stopped by separating the apical plate from the basolateral plate. Samples were collected from the receiver and donor compartments for analysis of PF-07321332 and internal standard by liquid chromatography tandem mass spectrometry (LC-MS/MS). Data for Caco-2 assays were analyzed using Analyst version 1.6.3 (Sciex, Framingham, MA) and the resulting peak areas of PF-07321332 and internal standard were determined. The concentrations of test compound were calculated based on the results of the standard curves. A-B P_{app} values were calculated using Microsoft Excel 2007 software.

In Vitro Transport Assays for BCRP and MDR1. The human BCRP-transfected MDCKII cell line (BCRP-MDCKII) and the human MDR1-transfected MDCKI cell line (MDR1-MDCKI) and were licensed from MilliporeSigma (Atlanta, GA) and the National Institutes of Health (Rockville, MD), respectively. Detailed procedures for the transwell assay have been used as described previously (Feng et al., 2019). In brief, BCRP-MDCKII cells were seeded at a cell density of 2.5 × 10^4 cells/well in complete minimum essential medium α containing 10% fetal bovine serum with supplements (1% GlutaMAX™, 1% penicillin-streptomycin and 1% non-essential amino acids) on Millicell-96 Cell Culture Insert Plates, and incubated (37 °C, 5% CO_2, 90% relative humidity) for 5 days. MDR1-MDCKI cells were seeded at a cell density of 3.4 × 10^4 cells/well in complete Dulbecco's modified Eagle's medium high glucose containing 10% fetal bovine serum with supplements (1% GlutaMAX™, 1% penicillin-streptomycin and 1% sodium pyruvate) on Millicell-96 Cell Culture Insert Plates, and incubated (37 °C, 5% CO_2, 90% relative humidity) for 4 days. All transwell assays were performed with transport buffer (HBSS

with 0.139 g/l calcium chloride, 25 mM D-glucose, 20 mM 4-(2-hydroxyethyl) piperazine-1-ethanesulfonic acid, and 0.102 g/l magnesium chloride) at pH 7.4. Transport assays were performed by adding PF-07321332 (0.3, 1, and 3 μM) and positive controls (0.5 μM of pitavastatin for BCRP and 0.5 μM of quinidine for MDR1) in transport buffer to donor wells and measuring appearance in receiver wells after a 1.5 h incubation at 37 °C. Samples were collected from the receiver and donor compartments for analysis by LC-MS/MS. The following equations were used to calculate P_{app} values and MDR1 or BCRP efflux ratio.

$$P_{app} = \frac{1}{A \times C_0} \bullet \frac{dx}{dt}$$

$$\text{Efflux ratio} = \frac{P_{app,BA}}{P_{app,AB}}$$

Where, A is the surface area of the transwell insert, C_0 is the initial concentration of a compound applied to the donor chamber, *t* is incubation time, *x* is the amount of a compound in the receiver compartment, and d*x*/d*t* is the flux of the compound across the cell monolayer.

Plasma Protein Binding. Plasma protein binding was determined using a 96-well equilibrium dialysis method (Banker et al., 2003). On the day of each incubation, fresh blood in K2EDTA was collected from male Wistar-Hannover rats (*n*=5, pooled), male Cynomolgus monkeys (*n*=2, pooled), and humans (*n*=1 male and *n*=1 female, pooled). The blood was centrifuged (10 min, 2500 x g) to harvest plasma. Plasma was spiked with a final concentration of 0.3, 1, 3, or 10 μM of PF-07321332 (final organic 1% DMSO). Fraction unbound in plasma ($f_{u,p}$) was determined by equilibrium dialysis using an HTD 96 device assembled with 12-14k molecular weight cutoff membranes (HTDialysis, LLC, Gales Ferry, CT). Dialysis chambers were loaded with 150 μl plasma and 150 μl phosphate buffered saline in the donor and receiver chambers, respectively. The dialysis plate was sealed with a gas-permeable membrane and stored in a 37 °C water-jacketed incubator maintained at 75% relative humidity and 5% CO_2, on a 100 rpm plate shaker. After a 6-hour incubation, samples were matrix-matched and quenched by protein precipitation, followed by analysis of PF-07321332 by LC-MS/MS. A set of satellite samples was included to measure stability after a 6-hour incubation. Incubations were conducted with 12 replicates per concentration. The unbound plasma fraction of PF-07321332 was calculated by dividing the

analyte concentration in the buffer sample by the concentration in the donor sample, corrected for any dilution factors. All incubations had >70% analyte recovery and >70% stability in 6 h.

Human Liver Microsomal Binding. Unbound fraction of PF-07321332 in human liver microsomes (HLM) ($f_{u,mic}$) was determined in quadruplicate using 96-well equilibrium dialysis. HLM were thawed and diluted with 0.1 M potassium phosphate buffer (pH 7.4) to a final protein concentration of 1 mg/ml. PF-07321332 (final concentration = 2 µM) was added to the diluted microsomal solution (final organic 1% DMSO). Dialysis chambers were loaded with 150 µl HLM and 150 µl 0.1 M potassium phosphate buffer (pH 7.4) in the donor and receiver chambers, respectively. The remainder of the study was conducted using the methods described for plasma protein binding. HLM binding was scaled to desired protein concentration using the following (Austin et al, 2002), where fu_1 is the measured fraction unbound at a first microsomal concentration (C_1) and f_{u2} is the calculated fraction unbound at a second microsomal concentration (C_2).

$$= \frac{1}{\frac{C_2}{C_1}\left(\frac{1-fu_1}{fu_1}\right)+1}$$

Blood to Plasma Ratio (BPR) Determination. Blood to plasma partitioning (R_b) of PF-07321332 was determined in fresh rat, monkey, and human whole blood that was collected in K_2EDTA. A 0.2 mM stock of PF-07321332 was prepared in 50% acetonitrile 50% water which was added to blood to yield a final concentration of 1 µM (*n* = 3, final organic 0.25% acetonitrile). An aliquot of blood was immediately removed for the stability determination. Samples were incubated on an orbital shaker in a humidified CO_2 incubator for 60 min at 37 °C. Post incubation, a whole blood sample was collected. The remaining blood samples was centrifuged for 10 min at 2500 x g and a plasma sample was collected. Each sample was matrix matched with an equal volume of blank plasma or blood, followed by dilution with 1.25 volumes of water. The resulting sample (90 µl) was mixed with 200 µl of 50% acetonitrile 50% methanol containing an internal standard (5 ng/ml terfenadine). Supernatants were analyzed for PF-07321332 using LC-MS/MS. The BPR for PF-07321332 was calculated as the ratio of PF-07321332 concentration in the blood to concentration in the plasma. All incubations had >70% analyte recovery in 1 h.

Microsomal Stability. *Liver.* PF-07321332 (0.1 μM) was incubated in Wistar-Han rat (male and female), Cynomolgus monkey (male), and HLM (pool of 50 donors of mixed gender) purchased from Sekisui XenoTech (Kansas City, KS) (1 mg/ml) in potassium phosphate buffer (100 mM, pH 7.4) supplemented with $MgCl_2$ (3.3 mM) and β-Nicotinamide adenine dinucleotide phosphate, reduced form (NADPH) (1.3 mM) in a final volume of 400 μl. Stock solutions of PF-07321332 were prepared in acetonitrile (final concentration of acetonitrile in the incubations were ≤ 0.5%). Incubations were conducted at 37 °C in triplicate. Control incubations in the absence of NADPH were also conducted in parallel in duplicate. Periodic aliquots (40 μl) of the incubation mixture at 0, 5, 10, 15, 20, 30, 45 and 60 min were removed and quenched in acetonitrile (160 μl) containing diclofenac (25 ng/ml) as internal standard.

Intestine. PF-07321332 (1.0 μM) was incubated in phenylmethylsulfonyl fluoride-free (to preserve serine hydrolase enzymatic activity) rat (pool of 200, male Sprague-Dawley), (Sekisui XenoTech, Kansas City, KS), monkey (pool of 10, male cynomolgus) or human (pool of 9, male and female) (BioIVT, Baltimore, MD) intestinal microsomes (1 mg/ml) in potassium phosphate buffer (100 mM, pH 7.4) supplemented in $MgCl_2$ (3.3 mM) and NADPH (1.3 mM) in a final volume of 300 μl. The final acetonitrile concentrations in the incubations were ≤ 0.5%. Incubations were conducted at 37 °C in duplicate. Control experiments in the absence of NADPH were also conducted in parallel. Periodic aliquots (30 μl) of the incubation mixture at 0, 5, 15, 30, 60, 90 and 120 min were added to acetonitrile (120 μl) containing diclofenac (25 ng/ml) as internal standard.

Samples from the microsomal stability assays were vortexed, centrifuged (5 min, 2300 x g), and the supernatant was diluted with an equal volume of water. Samples were analyzed for depletion of PF-07321332 by LC-MS/MS. Analyst software (Sciex, Framingham, MA) was used to measure peak areas. Peak area ratios of analyte to internal standard were calculated. PF-07321332 depletion half-life ($t_{1/2}$) and apparent intrinsic clearance ($CL_{int,app}$) were calculated using E-WorkBook v10 (ID Business Solutions, Guildford, Surrey, UK). The natural log of peak area ratios versus time were fitted using linear regression, and the slope (k) was converted to $t_{1/2}$ values, where $t_{1/2} = -0.693/k$. To estimate $CL_{int,app}$ in liver microsomes, the $t_{1/2}$ for substrate depletion was scaled using the following equation (Obach et al., 1997).

$$CL_{int,app} = \frac{0.693 \cdot ml\ incubation}{t_{\frac{1}{2}} \cdot amount\ of\ protein\ in\ incubation}$$

The following equations were used to calculate scaled intrinsic clearance ($CL_{int,scaled}$) and hepatic blood clearance ($CL_{hep,blood}$) in liver microsomes from animals and human. The physiological constants for each species used were 40 g liver/kg body weight and Q of 70 ml/min/kg (rat), 32 g liver/kg body weight and Q of 44 ml/min/kg (monkey), and 21 g liver/kg body weight and Q of 20 ml/min/kg (human) (Davies and Morris, 1993). $f_{u,mic}$ measured in HLM was used as a surrogate for all species (Zhang et al., 2010).

$$CL_{int,scaled} = CL_{int,app} \cdot \frac{45\ \text{mg microsomes}}{g\ liver} \cdot \frac{g\ liver}{kg\ body\ weight}$$

$$CL_{hep,blood} = \frac{\text{Q} \cdot \frac{f_{u,p}}{R_b} \cdot \frac{CL_{int,scaled}}{f_{u,mic}}}{\text{Q} + \frac{f_{u,p}}{R_b} \cdot \frac{CL_{int,scaled}}{f_{u,mic}}}$$

Hepatocyte metabolic stability. Cryopreserved Wistar-Han rat (male, pool of 24 donors), cynomolgus monkey (male, pool of 3 donors), and human (pool of 13 donors of mixed gender) hepatocytes were purchased from BioIVT (Baltimore, MD). Hepatocytes were suspended at 0.5 x 10^6 viable cells/ml of Williams E media and prewarmed at 37 °C for 30 min. Incubations were initiated with the addition of PF-07321332 (final concentration = 1.0 μM, final DMSO concentration = 0.1%) and were conducted at 37 °C, 75% relative humidity, and 5% CO_2. The reaction was stopped at 2, 4, 11, 45, 75, 120, or 240 min by the addition of acetonitrile (135 μl) containing a proprietary internal standard CP-628374 (0.177 μM). The samples were centrifuged at ~1900 × *g* for 5 min before LC-MS/MS analysis for the depletion of PF-07321332 in the incubations. The following equations were used to calculate $CL_{int,app}$, $CL_{int,scaled}$, and $CL_{hep,blood}$ (Di et al., 2012). The physiological constants for each species used were 135 x 10^6 cells/g liver (rat), 120 x 10^6 cells/g liver (monkey), and 120 x 10^6 cells/g liver (human).

$$Hepatocyte\ CL_{int,app} = \frac{0.693}{t_{\frac{1}{2}}} \cdot \frac{ml\ incubation}{million\ cells}$$

$$Hepatocyte\ CL_{int,\text{scaled}} = Hepatocyte\ CL_{int,app} \cdot \frac{million\ cells}{g\ liver} \cdot \frac{g\ liver}{kg\ body\ weight}$$

$$CL_{hep,blood} = \frac{\mathrm{Q} \cdot \frac{f_{u,p}}{R_b} \cdot \frac{CL_{int,scaled}}{f_{u,mic}}}{\mathrm{Q} + \frac{f_{u,p}}{R_b} \cdot \frac{CL_{int,scaled}}{f_{u,mic}}}$$

LC-MS/MS Analysis of PF-07321332 from In Vitro Studies. LC-MS/MS analysis was performed using a Sciex Triple Quad 6500 mass spectrometer (Sciex, Framingham, MA), equipped with an electrospray source and Agilent 1290 binary pump (Santa Clara, CA). Aqueous mobile phase (A) was comprised of 0.1% formic acid in water and organic mobile phase (B) consisted of 0.1% formic acid in acetonitrile. Samples (10 µl) from various in vitro incubations were injected onto a Kinetex XB-C18 (2.1 x 50 mm, 2.6 µm) (Phenomenex, Torrance, CA) column at room temperature with a flow rate of 0.5 ml/min. The gradient program typically began with 10% initial mobile phase B held for 0.2 min, followed by a linear gradient to 40% B over 2.3 min, then to 98% over 0.3 min, held at 98% B for 0.6 min followed by re-equilibration to initial conditions for 0.3 min. The mass spectrometer was operated in multiple reaction monitoring mode, in positive detection mode, with the mass transitions (Q1/Q3) and collision energies (CEs) of 500/110 and 30, respectively, for PF-07321332.

Preclinical Pharmacokinetics Studies. All activities involving animals were carried out in accordance with federal, state, local and institutional guidelines governing the use of laboratory animals in research in AAALAC accredited facilities and were reviewed and approved by Pfizer's or Bioduro's Institutional Animal Care and Use Committee.

Rat Pharmacokinetics. Rat pharmacokinetics studies were done at Pfizer (Groton, CT) or BioDuro Pharmaceutical Product Development Inc. (Shanghai, PRC); Jugular vein-cannulated male Wistar-Hannover rats were purchased from Charles River Laboratories, Inc. (Wilmington, MA) or Vital River (Beijing, China) and were typically 7-10 weeks of age at the time of dosing. During the pharmacokinetic studies all animals were housed individually. Access to food and water was provided ad libitum (i.e., subjects were dosed in the fed state). PF-07321332 was administered intravenously (iv) via the tail vein (n = 2 or 3) dosed as a solution (1 mg/kg, 1 ml/kg) or via oral (po) gavage as a solution or suspension (10 mg/kg, 10 ml/kg). Intravenous doses for PF-07321332 were administered as a solution in 10% DMSO/30% PEG400/60% deionized water. An iv dose of PF-07321332 (1 mg/kg) was also administered to bile duct-cannulated Sprague-Dawley rats (n=4), where plasma, bile, and urine samples were collected on

ice for up to 24 hours and stored at – 20 °C until analysis. Serial blood samples from rat pharmacokinetics studies were collected before dosing and 0.033, 0.083, 0.25, 0.5, 1, 2, 4, 7, and 24 hours after dosing. Oral (po) rat pharmacokinetics studies were conducted with crystalline PF-07321332 methyl-tert-butyl ether (MTBE) solvate or anhydrous 'Form 1'. PF-07321332-MTBE solvate and anhydrous 'Form 1' forms were formulated as solutions in 10% (v/v) ethanol/10% (v/v) capmul MCM/35% (v/v) PEG400/45% (v/v) polysorbate and 2% (v/v) tween80/98% of 0.5% (w/v) methyl cellulose in deionized water, respectively. Rats received 8 ml/kg oral of 1% Hydroxypropyl cellulose in deionized water immediately prior to the PF-07321332-MTBE solvate po dose. Serial blood samples were collected via the jugular vein cannula at predetermined timepoints after dosing. Urine samples (0–7.0 and 7.0–24 h) were also collected after iv administration. At the completion of the study, animals were euthanized by overdose of inhaled anesthesia followed by exsanguination. Blood samples were collected into tubes containing K_2EDTA and stored on ice until centrifugation to obtain plasma, which was stored frozen at -20 °C or lower.

Monkey Pharmacokinetics. Monkey studies were conducted at Pfizer (Groton, CT). Male Cynomolgus monkeys were purchased from Covance (Princeton, NJ), Charles River Laboratories, Inc. (Wilmington, MA), or Envigo Global Services (Indianapolis, IN); subjects 3-8 years of age were used in pharmacokinetics studies. For each study (n=2), PF-07321332 was dosed iv by the saphenous vein (typically 1 mg/kg and 1 ml/kg) or via po gavage (typically 5–10 mg/kg, 5 ml/kg). For iv studies, PF-07321332 was administered as a solution in 5% (v/v) PEG400:95% (v/v) of 23% 2-hydroxypropyl-β-cyclodextrin in aqueous sodium phosphate buffer pH = 6.0. For po studies, crystalline MTBE solvate form of PF-07321332 was administered as a solution in 2% (v/v) tween80/98% of 0.5% (w/v) methyl cellulose in deionized water. Serial blood samples were collected via the femoral vein before dosing and at predefined time points post-dose. Urine samples (0–7.0 and 7.0–24 h) were also collected after iv administration. Blood samples were collected into K_3EDTA treated collection tubes and were stored on wet ice prior to being centrifuged to obtain plasma, which was stored frozen at - 20 °C or lower.

LC-MS/MS Analysis. Bile and urine samples were diluted 1:9 in plasma. Plasma, bile or urine samples were processed using protein precipitation with 1:1 acetonitrile:methanol containing terfenadine (5 ng/ml) or buspirone (5 ng/ml) as an internal standard followed by quantitation

against a standard curve (0.1-2500 ng/ml) prepared in blank plasma. Briefly, a Waters ACQUITY ultra performance liquid chromatography system (Waters, Milford, MA) coupled to an Sciex 6500 triple quadrupole mass spectrometer equipped with an electrospray ionization source was used. Chromatographic separation was accomplished using a Waters Acquity UPLC BEH C18 column (1.7 µm, 2.1 × 50 mm) maintained at either room temperature or 45 °C. The mobile phase (2 solvents gradient) was optimized to achieve good separation between the analytes. Typically, solvent A constituted of 0.1% formic acid in water, and solvent B included 0.1% formic acid in acetonitrile. The gradient generally began at 5-30% B until about 1 min, followed by an increase to 95% B to 2.0 min and held for 0.5 min, then decreased to 5-30% B until ~2.6 min. MS/MS methods were the same as described for in vitro samples. Analyst v.1.7 software was used for peak integration and Watson v.7.5 (Thermo Scientific, Waltham, MA) was used for standard curve regression.

Pharmacokinetic Analysis. Pharmacokinetic parameters were calculated using noncompartmental analysis (Watson v.7.5). The area under the plasma concentration-time curve from t = 0 to infinity (AUC0-∞) was estimated using the linear trapezoidal rule. In some instances, pharmacokinetic calculations were generated using the linear log-linear trapezoidal rule and C_0 was calculated using the equation:

$$C_0 = \frac{Dose_{iv}}{V_b \times BPR}$$

where V_b is the blood volume (rat, 69.0 ml/min/kg; monkey, 62.3 ml/kg) and BPR is the blood to plasma ratio. Plasma clearance (CL_p) was calculated as:

$$CL_p = \frac{Dose_{iv}}{AUC_{0-\infty}}$$

The terminal rate constant (k_{el}) was calculated by linear regression of the terminal phase of the log-linear concentration-time curve and the terminal elimination $t_{1/2}$ was calculated as:

$$t_{\frac{1}{2}} = \frac{0.693}{k_{el}}$$

Steady state distribution volume (Vd_{ss}) was determined by clearance multiplied by mean residence time. Oral bioavailability (F) was defined as:

$$F = \frac{AUC_{po} \times Dose_{iv}}{AUC_{iv} \times Dose_{po}}$$

The fraction of the oral dose absorbed (F_a x F_g) was estimated using the equation (Kato et al., 2003):

$$F_a \times F_g = \frac{F}{1 - \frac{CL_{blood}}{Q}}$$

A hepatic blood flow (Q) of 70 ml/min/kg and 44 ml/min/kg was used for rats and monkeys, respectively (Davies and Morris, 1993). Blood clearance (CL_{blood}) was calculated by dividing CL_p by the blood-to-plasma ratio in the respective preclinical species.

The total amount of PF-07321332 excreted unchanged in urine or bile was calculated using the following equations and summing the amount in all collection intervals, where C_u and C_b are the measured urine and bile concentrations, respectively, DF is the dilution factor applied during bioanalysis, and V_u and V_b are the volumes of urine and bile collected during each time interval.

$$Amount\ in\ Urine = C_u \times DF \times V_u$$

$$Amount\ in\ Bile = C_b \times DF \times V_b$$

Renal clearance (CL_{renal}) and biliary clearance ($CL_{biliary}$) were calculated as:

$$CL_{renal} = \frac{Amount\ in\ urine}{Amount\ dosed} \times CL_p$$

$$CL_{biliary} = \frac{Amount\ in\ bile}{Amount\ dosed} \times CL_p$$

CYP Inhibition Studies. Reversible inhibition of major human CYP isoforms (CYP1A2, CYP2B6, CYP2C8, CYP2C9, CYP2C19, CYP2D6, and CYP3A4/5) by PF-07321332 was evaluated via incubation of standard marker substrates (phenacetin (CYP1A2), bupropion (CYP2B6), amodiaquine (CYP2C8), diclofenac (CYP2C9), *S*-mephenytoin (CYP2C19), dextromethorphan (CYP2D6), testosterone (CYP3A4/5), midazolam (CYP3A4/5), and nifedipine (CYP3A4/5)) of human CYP isozymes with pooled HLM in the presence of NADPH (1.3 mM) in 100 mM potassium phosphate buffer, pH 7.4, containing 3.3 mM $MgCl_2$ at 37 °C open to air. The incubation volume was 0.2 ml. Microsomal protein concentrations, substrate concentrations, incubation times, and reaction termination solvents for each activity have been

described in detail previously (Walsky and Obach, 2004). Incubation mixtures contained PF-073231332 at concentrations ranging from 0.01–300 μM. Stock solutions of PF-07321332 were prepared in 90% acetonitrile 10% water. The final concentration of acetonitrile in the incubation mixtures was 0.9% (v/v). Parallel incubations were conducted to determine the IC_{50} after a 30 min preincubation (IC_{50} shift) (Perloff et al., 2009), where PF-07321332 was incubated with HLM and NADPH for 30 min prior to the co-incubation with marker substrate. Time dependent inhibition occurred when the IC_{50} was ≥ 1.5 more potent after preincubation. Nonlinear regression was performed in GraphPad to determine the IC_{50} using the following equation, where Y is the percent activity remaining, [I] is the inhibitor concentration, and Hill Slope was determined based on the fit of the data (typically 1).

$$Y = \frac{100}{1 + 10^{(\log[I] - \log(IC50)) \cdot \mathrm{HillSlope}}}$$

To examine the ability of PF-07321332 to act as a time- and/or NADPH-dependent inhibitor of CYP3A, incubations were conducted in HLM (0.3 mg/ml) supplemented with $MgCl_2$ (3.3 mM) and NADPH (1.3 mM) in potassium phosphate buffer (100 mM, pH 7.4). PF-07321332 stock solutions, at concentrations of 0.1-100 μM (final), were prepared at 100-times the final incubation concentration in a mixture of 90% acetonitrile 10% water (final organic 0.9% acetonitrile). The incubation was initiated with the addition of PF-07321332 stock solution to the microsomal mixture. Periodic aliquots (1–40 min) of the mixture was transferred to an activity incubation mixture containing midazolam (20.9 μM, 10-fold K_M), $MgCl_2$ (3.3 mM), and NADPH (1.3 mM) in potassium phosphate buffer (100 mM, pH 7.4), resulting in a 20-fold dilution. After 6 min, the activity reaction was terminated by the addition of two volumes of acetonitrile containing internal standard (100 ng/ml [$^2H_4$]1'-hydroxymidazolam). Reactions were carried out at 37 °C, at a final volume of 200 μl, in duplicate. Samples were vortexed and centrifuged for 5 min at approximately 2300 x *g* at room temperature. The supernatant was mixed with an equal volume of water containing 0.2% formic acid and analyzed directly by LC-MS/MS. LC-MS/MS analysis was conducted on a Sciex 6500 triple quadrupole mass spectrometer fitted with an electrospray ion source operated in positive ion mode using multiple reaction monitoring. An Agilent 1290 binary pump with a CTC Leap autosampler (Leap Technology, Carrboro, NC) was programmed to inject 10 μl of sample on a Halo 2.7 μm C18 2.1x30 mm column (Advanced Materials Technology, Wilmington, DE). A binary

gradient was employed using 0.1% (v/v) formic acid in water (mobile phase A) and 0.1% (v/v) formic acid in acetonitrile (mobile phase B) at a flow rate of 0.5 ml/min. Mass-to-charge (*m/z*) transitions (Q1/Q3) for analytes 1'-hydroxymidazolam and [$^2H_4$]1'-hydroxymidazolam were 342.2/324.2 and 346.2/328.2, respectively. To determine the kinetic inactivation parameters, the natural log of percent remaining activity versus preincubation time was plotted then the slope of the line ($-k_{obs}$) was calculated using linear regression. K_I and k_{inact} parameters were determined using nonlinear regression of the three-parameter Michaelis-Menten equation below:

$$k_{obs} = k_{obs[0\mu M]} + \frac{k_{inact} \times [I]}{K_I + [I]}$$

[I] represents the concentrations of the test drug in the primary incubation, k_{inact} is the maximal inactivation rate, $k_{obs[0\ \mu M]}$ is the inactivation rate in the solvent control, and K_I is the inactivator concentration at half k_{inact}. A similar experiment was conducted using testosterone as the CYP3A probe substrate. These incubations contained testosterone in the activity incubation mixture at 10-fold K_M (386 µM) which was carried out for a duration of 10 min. The internal standard solution contained 100 ng/ml [$^2H_3$]6β-hydroxytestosterone. Mass-to-charge (*m/z*) transitions (Q1/Q3) for analytes 6β-hydroxytestosterone and [$^2H_3$]6β-hydroxytestosterone were 305.2/269.2 and 308.2/272.7, respectively, and analytes were separated using a Halo 2 µm C18 2.1x50 mm column.

Measurement of absorption spectra of CYP metabolic intermediate (MI) complexes. Aliquots of recombinant human CYP3A4, oxidoreductase, cytochrome b5 supersomes (Corning, 0.3 nmol/ml final CYP concentration) and NADPH (1 mM final concentration) in 0.1 M potassium phosphate buffer containing 3.3 mM magnesium chloride (pH 7.4) were transferred to matched sample and reference cuvettes (990 µl each) in a Agilent Cary Series 100 UV-Vis spectrophotometer (Santa Clara, CA). The instrument was zeroed and baselined between 400 and 500 nm. Reactions were started by addition of 10 µl of 1 mM acetonitrile solutions of either troleandomycin (CYP3A4 inactivator and positive control) or PF-07321332 to the sample cuvette and 10 µl of acetonitrile to the reference cuvette. Spectral scans (400–500 nm) were at approximately 0, 1, 5, 10, 15, 20, 25, and 30 min.

CYP3A4 Induction in Human Hepatocytes. Cryopreserved human hepatocytes were used to examine CYP3A4 induction potential of PF-07321332 using established protocols (Dong et al.,

2017). Briefly, primary cultures of human hepatocytes from four donors (BXM, BNA, FOS, and HH1144) were seeded in collagen I-precoated 24-well plates, and each well had a cell density of ~ 7.0 x 10^5 viable cells. Hepatocyte cultures were treated for 2 consecutive days with medium containing solvent (0.1% DMSO) control, PF-07321332 (0.01, 0.03, 0.1, 0.3, 1.0, 3.0, 10, 30, 50, 100, and 200 μM), or prototypical CYP3A4 inducer rifampicin (10 μM). Following the incubation phase of the experiment, the medium containing test compounds or vehicle was removed and the cells were washed with phosphate buffered saline and fresh medium was added to all wells for a 30 minute wash. Following removal of the wash media, midazolam (30 μM) in 0.1% DMSO was added to each well and the plate was returned to the incubator for 30 minutes. After incubation, 200 μl of the medium from each well was removed and analyzed for 1-hydroxymidazolam formation using established LC-MS/MS protocols (Walsky and Obach, 2004). Quantification of CYP3A4 messenger RNA (mRNA) was performed using the TaqMan® as previously described (Fahmi et al., 2008). Data for mRNA and activity (normalized to DMSO vehicle control) were plotted versus the concentration of the PF-07321332 or rifampin. Individual fitting was carried out on each hepatocyte donor using GraphPad Prism (version 8.0.2), and was fit to either a four-parameter sigmoidal model (fitting maximum fold induction ($Ind_{max} = E_{max} + 1$), Hill slope (γ), and concentration of PF-07321332 that produced half Ind_{max} (EC_{50}), with baseline fixed at 1), three-parameter sigmoidal model (fitting Ind_{max} and EC_{50}, with Hill slope and baseline each fixed at 1), or a linear function (with y intercept fixed at 1); simpler models were preferred unless adding a parameter produced a fit with a p value < 0.05 by an extra sum-of-squares F test.

In Vitro Transporter Inhibition Assays. The inhibition of BCRP and MDR1 was measured using membrane vesicles (Solvo Biotechnology, Budapest, Hungary). Transporter-transfected human embryonic kidney (HEK)293 cells were used to measure the inhibition for organic anion transporting polypeptide (OATP)1B1 and 1B3 (Pfizer (Groton, CT) and Pfizer (sandwich, United Kingdom), respectively), multidrug and toxin extrusion protein (MATE)1/2K (Dr. Katsuhisa Inoue, Nagoya city University, Nagoya, Japan), organic cation transporter (OCT)1/2, and organic anion transporter (OAT)1/3 (Professor Kathleen Giacomini, University of California, San Francisco, CA). A 30-min pre-incubation with PF-07321332 or a control inhibitor was performed prior to the OATP1B1/1B3 assay incubation. The assays were started by adding probe substrates in the presence or absence of PF-07321332 (8 concentrations at 0.032-

1000 μM) and control inhibitors. The cells were incubated for 1-4 min depending on the transporter. The following probe substrates were used at concentrations below their K_m values; 0.2 μM of rosuvastatin for BCRP (K_m=3.2 μM) and 0.2 μM of *N*-methyl quinidine for MDR1 K_m=0.72 μM), 10 or 15 μM of metformin for MATE1/2K and OCT1/2 (K_m=1481-2596 μM), 0.5 μM of para- aminohippuric acid for OAT1 (K_m=4.97 μM), 0.1 μM of estrone-3-sulfate for OAT3 (K_m=9.46 μM), 0.3 μM of rosuvastatin for OATP1B1/1B3 (K_m=3.8/28.3 μM). Detailed procedures have been described previously (Bi et al., 2019; Boras et al., 2021; Costales et al., 2021). IC_{50} values for all transporters assays were estimated using the following equation from GraphPad Prism:

$$Percent\ Activity = Bottom + \frac{(Top - Bottom)}{1 + 10^{((logIC_{50} - [inhib]) * HillSlope)}}$$

References

Austin RP, Barton P, Cockroft SL, Wenlock MC, and Riley RJ (2002) The influence of nonspecific microsomal binding on apparent intrinsic clearance, and its prediction from physicochemical properties. *Drug Metab Dispos* **30:**1497-1503.

Banker MJ, Clark TH, and Williams JA (2003) Development and validation of a 96-well equilibrium dialysis apparatus for measuring plasma protein binding. *J Pharm Sci* **92:**967-974.

Bi YA, Costales C, Mathialagan S, West M, Eatemadpour S, Lazzaro S, Tylaska L, Scialis R, Zhang H, Umland J, Kimoto E, Tess DA, Feng B, Tremaine LM, Varma MVS, and Rodrigues AD (2019) Quantitative Contribution of Six Major Transporters to the Hepatic Uptake of Drugs: "SLC-Phenotyping" Using Primary Human Hepatocytes. *J Pharmacol Exp Ther* **370:**72-83.

Boras B, Jones RM, Anson BJ, Arenson D, Aschenbrenner L, Bakowski MA, Beutler N, Binder J, Chen E, Eng H, Hammond H, Hammond J, Haupt RE, Hoffman R, Kadar EP, Kania R, Kimoto E, Kirkpatrick MG, Lanyon L, Lendy EK, Lillis JR, Logue J, Luthra SA, Ma C, Mason SW, McGrath ME, Noell S, Obach RS, O' Brien MN, O'Connor R, Ogilvie K, Owen D, Pettersson M, Reese MR, Rogers TF, Rosales R, Rossulek MI, Sathish JG, Shirai N, Steppan C, Ticehurst M, Updyke LW, Weston S, Zhu Y, White KM, García-Sastre A, Wang J, Chatterjee AK, Mesecar AD, Frieman MB, Anderson AS, and Allerton C (2021) Preclinical characterization of an intravenous coronavirus 3CL protease inhibitor for the potential treatment of COVID19. *Nat Commun* Oct 18;12(1):6055. doi: 10.1038/s41467-021-26239-2.

Costales C, Lin J, Kimoto E, Yamazaki S, Gosset JR, Rodrigues AD, Lazzaro S, West MA, West M, and Varma MVS (2021) Quantitative prediction of breast cancer resistant protein mediated drug-drug interactions using physiologically-based pharmacokinetic modeling. *CPT Pharmacometrics Syst Pharmacol* Jun 24. doi: 10.1002/psp4.12672.

Davies B and Morris T (1993) Physiological parameters in laboratory animals and humans. *Pharm research* **10:**1093-1095.

Di L, Whitney-Pickett C, Umland JP, Zhang H, Zhang X, Gebhard DF, Lai Y, Federico JJ, 3rd, Davidson RE, Smith R, Reyner EL, Lee C, Feng B, Rotter C, Varma MV, Kempshall S, Fenner K, El-Kattan AF, Liston TE, and Troutman MD (2011) Development of a new permeability assay using low-efflux MDCKII cells. *J Pharm Sci* **100:**4974-4985.

Di L, Keefer C, Scott DO, Strelevitz TJ, Chang G, Bi YA, Lai Y, Duckworth J, Fenner K, Troutman MD, and Obach RS (2012) Mechanistic insights from comparing intrinsic clearance values between human liver microsomes and hepatocytes to guide drug design. *Eur J Med Chem* **57:**441-448.

Dong JQ, Gosset JR, Fahmi OA, Lin Z, Chabot JR, Terra SG, Le V, Chidsey K, Nouri P, Kim A, Buckbinder L, and Kalgutkar AS (2017) Examination of the human cytochrome P4503A4 induction potential of PF-06282999, an irreversible myeloperoxidase inactivator: Integration of preclinical, in silico, and biomarker methodologies in the prediction of the clinical outcome. *Drug Metab Dispos* **45:**501-511.

Fahmi OA, Boldt S, Kish M, Obach RS, and Tremaine LM (2008) Prediction of drug-drug interactions from in vitro induction data: application of the relative induction score approach using cryopreserved human hepatocytes. *Drug Metab Dispos* **36:**1971-1974.

Feng B, West M, Patel NC, Wager T, Hou X, Johnson J, Tremaine L, and Liras J (2019) Validation of Human MDR1-MDCK and BCRP-MDCK Cell Lines to Improve the Prediction of Brain Penetration. *J Pharm Sci* **108:**2476-2483.

Kato M, Chiba K, Hisaka A, Ishigami M, Kayama M, Mizuno N, Nagata Y, Takakuwa S, Tsukamoto Y, Ueda K, Kusuhara H, Ito K, and Sugiyama Y (2003) The intestinal first-pass metabolism of substrates of CYP3A4 and P-glycoprotein-quantitative analysis based on information from the literature. *Drug Metab Pharmacokinet* **18:**365-372.

Perloff ES, Mason AK, Dehal SS, Blanchard AP, Morgan L, Ho T, Dandeneau A, Crocker RM, Chandler CM, Boily N, Crespi CL, and Stresser DM (2009) Validation of cytochrome P450 time-dependent inhibition assays: a two-time point IC50 shift approach facilitates kinact assay design. *Xenobiotica* **39:**99-112.

Obach RS (1997) Nonspecific binding to microsomes: impact on scale-up of in vitro intrinsic clearance to hepatic clearance as assessed through examination of warfarin, imipramine, and propranolol. *Drug Metab Dispos* **25:**1359-1369.

Varma MV, Gardner I, Steyn SJ, Nkansah P, Rotter CJ, Whitney-Pickett C, Zhang H, Di L, Cram M, Fenner KS, and El-Kattan AF (2012) pH-Dependent solubility and permeability criteria for provisional biopharmaceutics classification (BCS and BDDCS) in early drug discovery. *Mol Pharm* **9:**1199-1212.

Walsky RL and Obach RS (2004) Validated assays for human cytochrome P450 activities. *Drug Metab Dispos* **32:**647-660.

Zhang Y, Yao L, Lin J, Gao H, Wilson TC, and Giragossian C (2010) Lack of appreciable species differences in nonspecific microsomal binding. *J Pharm Sci* **99:**3620-3267.

Supplemental Figure 1. ^{1}H NMR spectrum of PF-07321332.

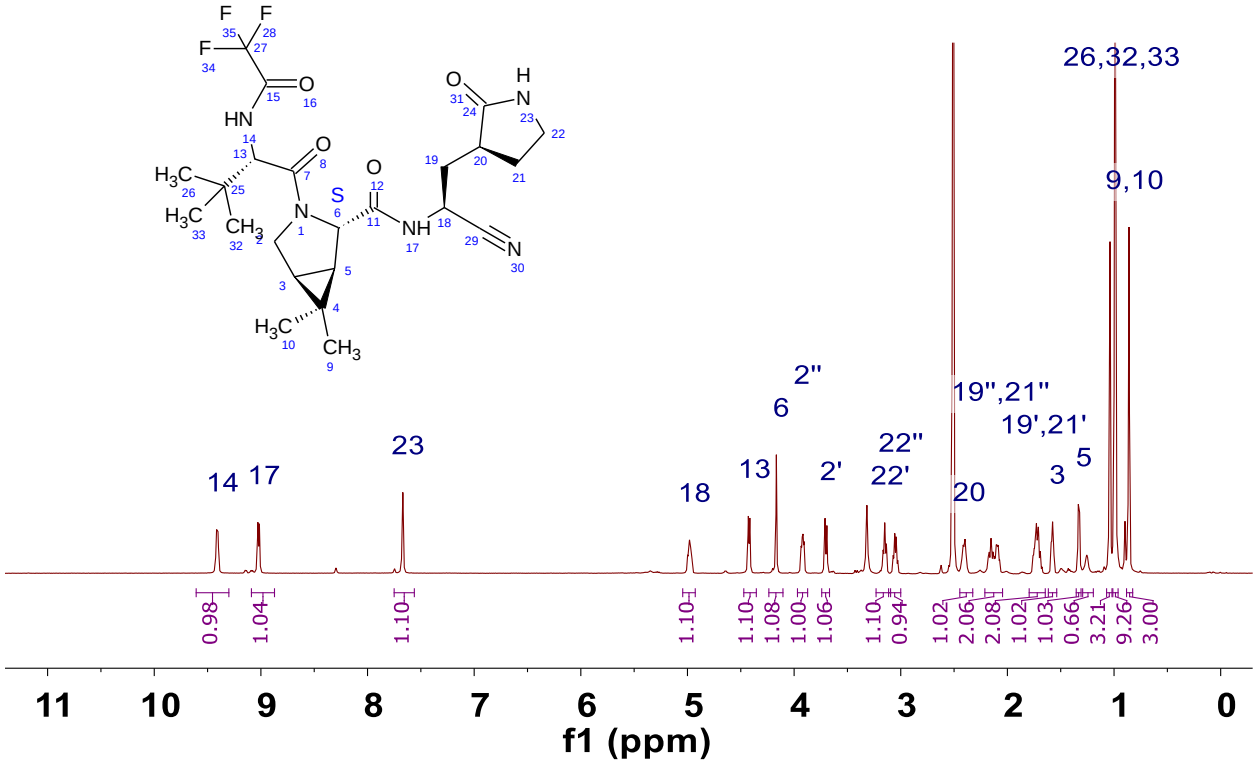

Supplemental Figure 2. High-resolution mass spectral data for metabolite M1 (PF-07329265). Top panel MS^1 spectrum; middle and lower panels are MS^2 spectra of *m/z* 516 from collision-induced dissociation (CID) and high-energy C-trap dissociation (HCD), respectively.

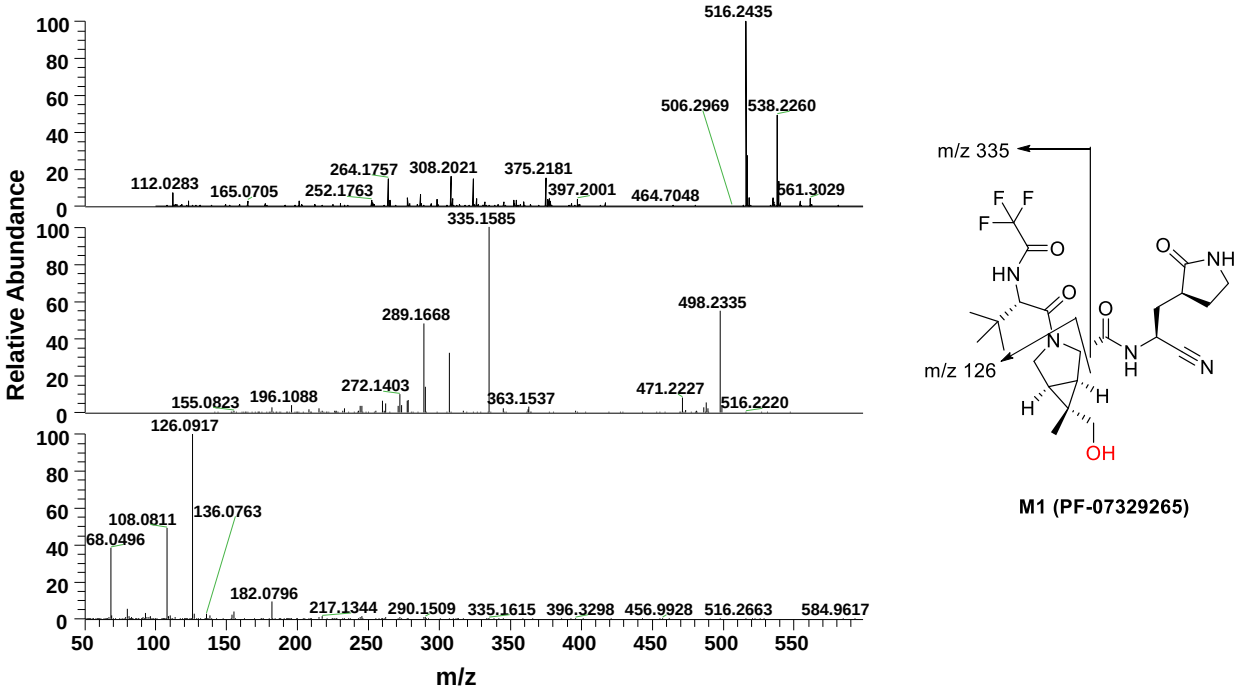

Supplementary Figure 3. ^{1}H NMR spectrum of M1 (PF-07329265).

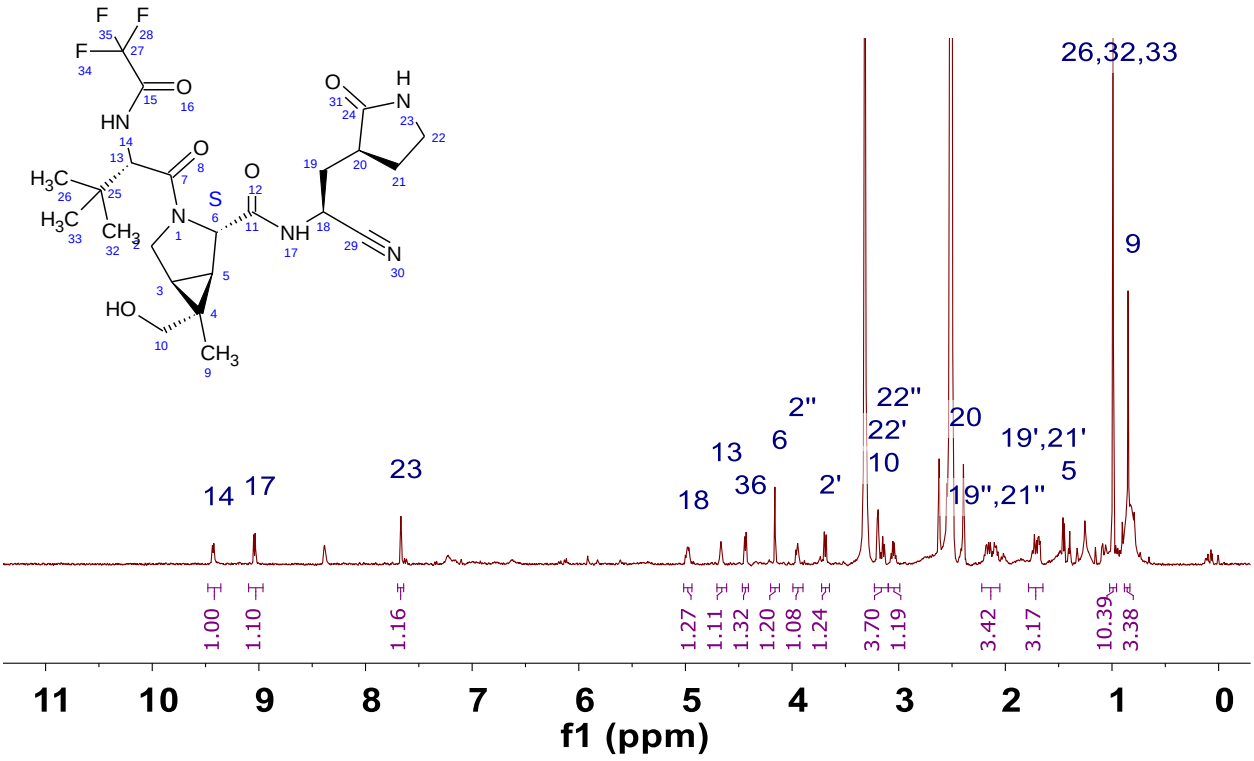

Supplementary Figure 4. Comparison of the ^{1}H-^{13}C HSQC of PF-07321332 (panel B) and M1 (PF-07329265) (panel C), ^{1}H NMR spectrum of PF-07329265 at 340 °K (panel D), 1D ROE spectra of PF-07329265 at 340 °K, C10 methylene irradiated, δ 3.32, (panel E), 1D ROE spectrum of PF-07329265 at 340 °K, C9 methyl irradiated, δ 0.86 (panel F).

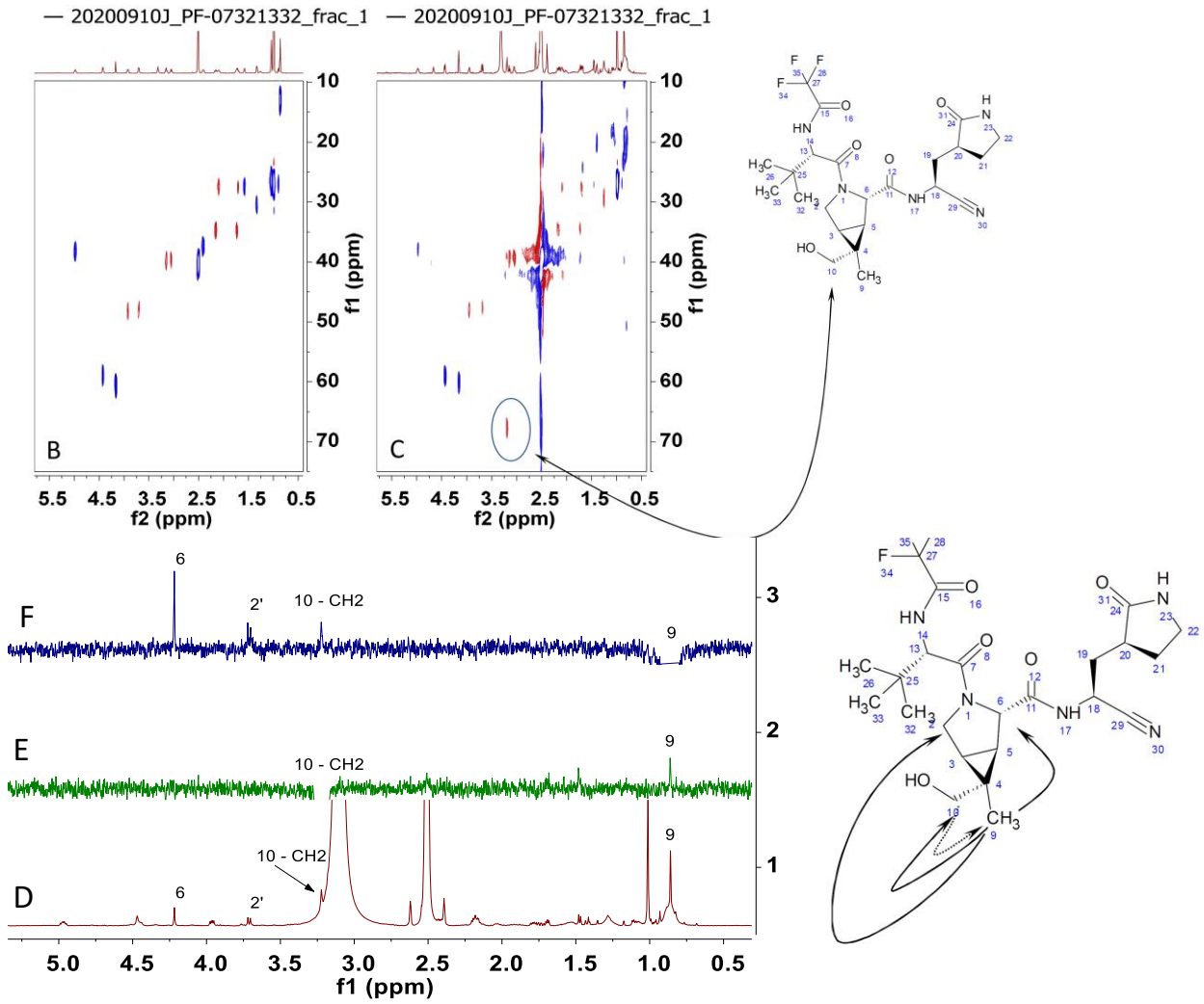

Supplementary Figure 5. Energy minimized three dimensional structure of metabolite M1 (PF-07329265).

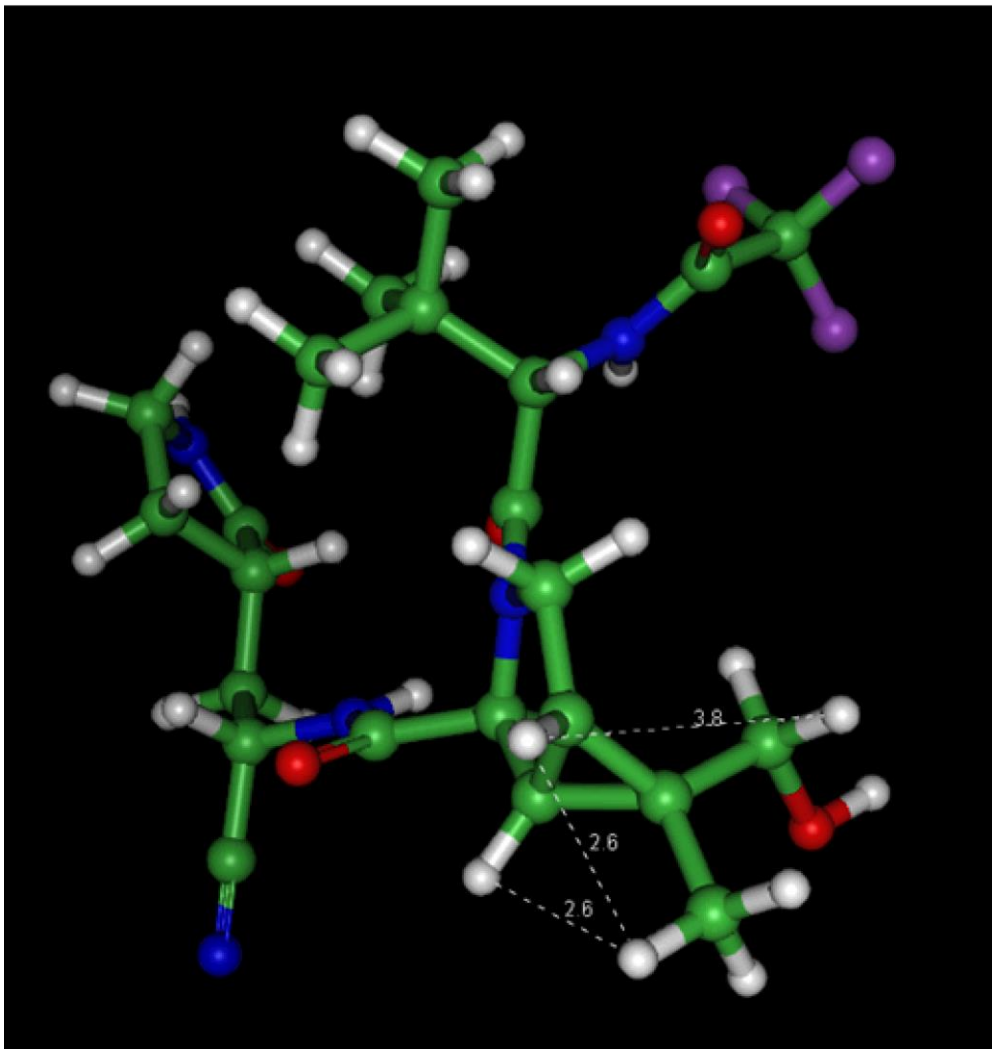

Supplemental Figure 6. High-resolution mass spectral data for metabolite M2 (PF-07329266). Top panel MS^1 spectrum; middle and lower panels are MS^2 spectra of *m/z* 516 from CID and HCD, respectively.

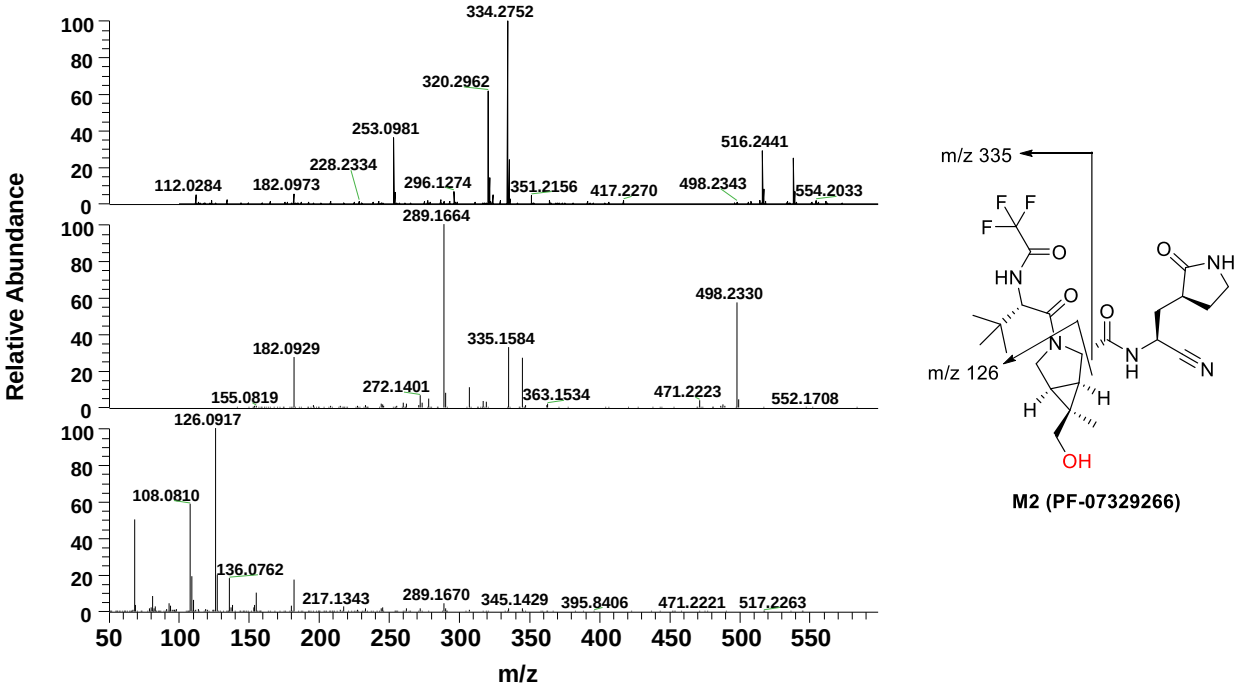

Supplementary Figure 7. ^{1}H NMR spectrum of metabolite M2 (PF-07329266).

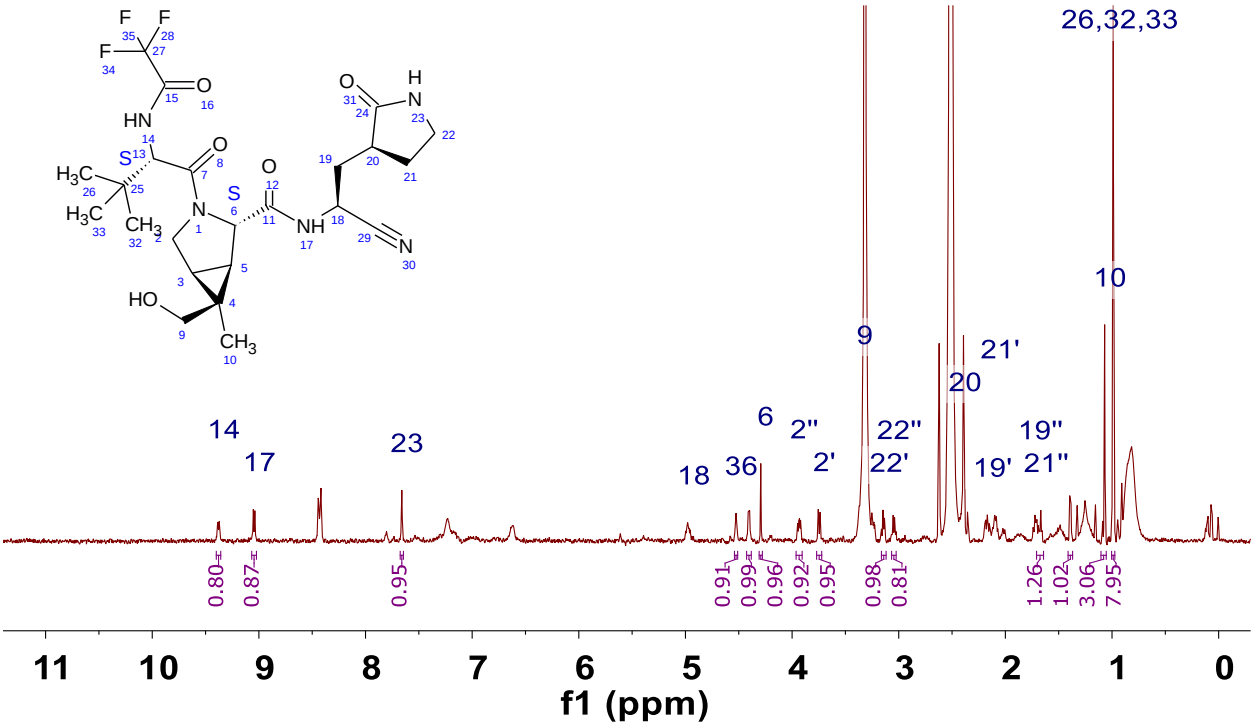

Supplementary Figure 8. High-resolution mass spectra data for metabolite M3 (PF-07329267). Top panel MS^1 spectrum; middle and lower panels are MS^2 spectra of *m/z* 516 from CID and HCD, respectively.

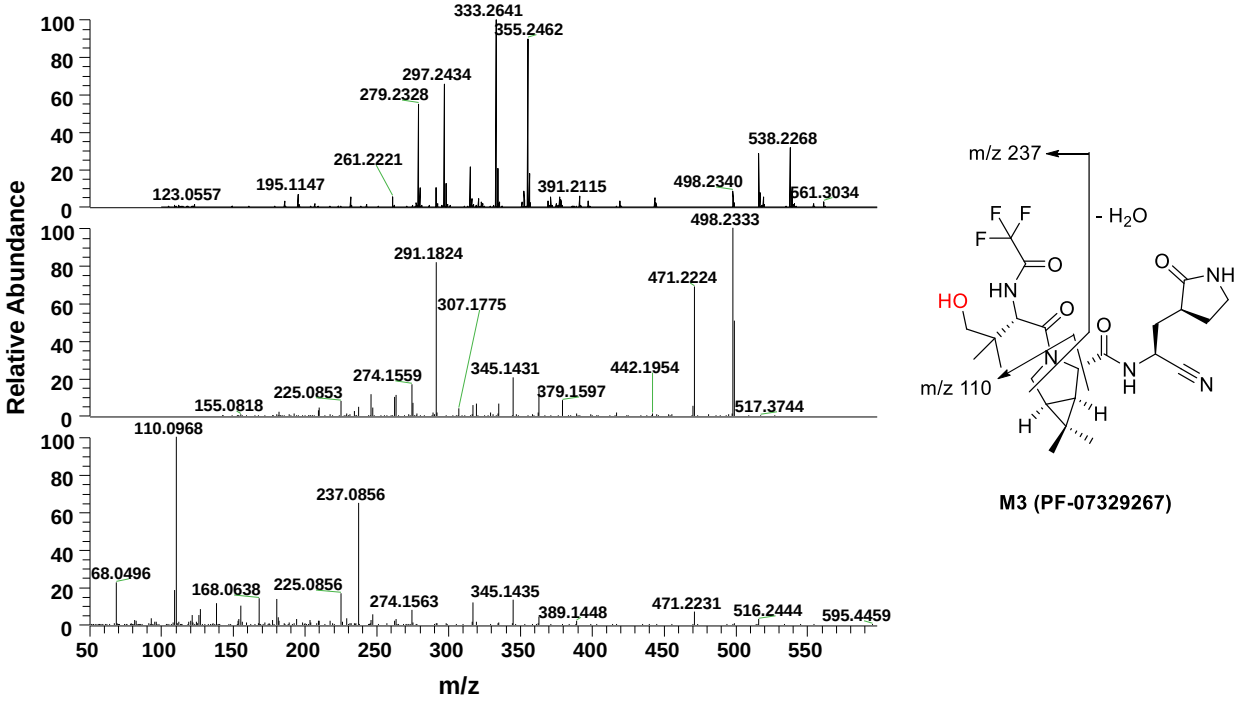

Supplementary Figure 9. ^{1}H NMR spectrum of metabolite M3 (PF-07329267).

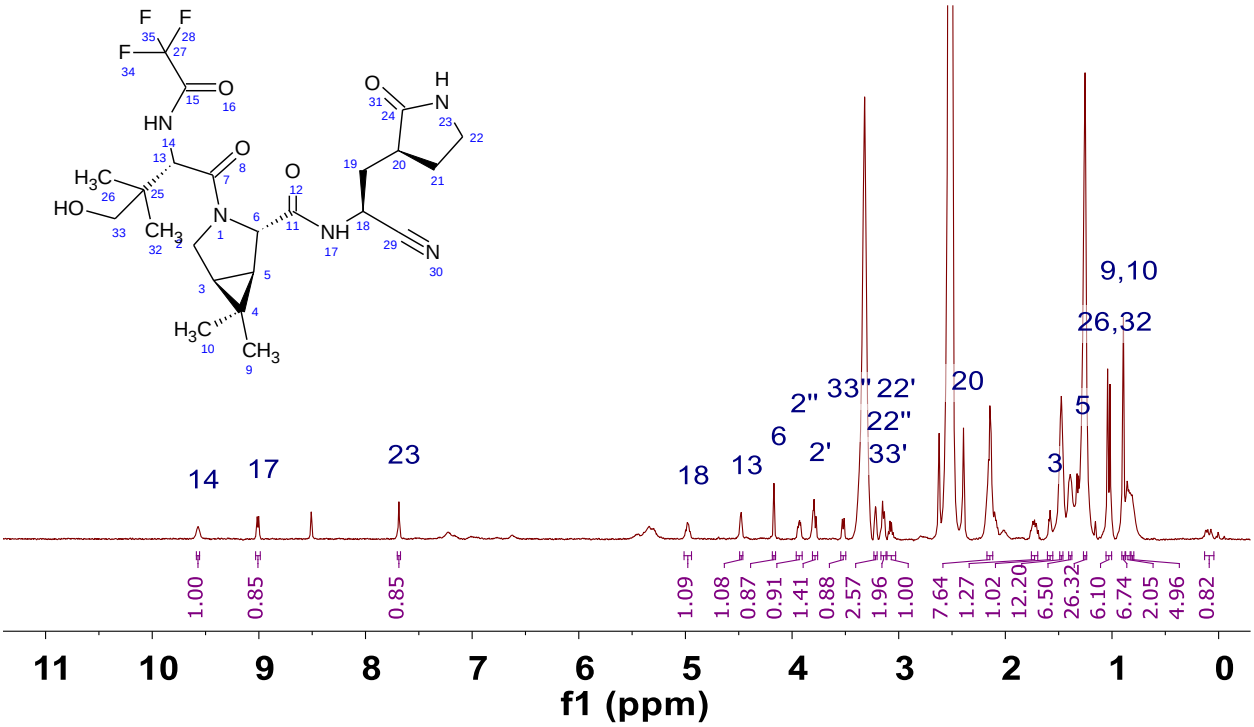

Supplementary Figure 10. ^{1}H-^{13}C HSQC NMR spectrum of metabolite M3 (PF-07329267).

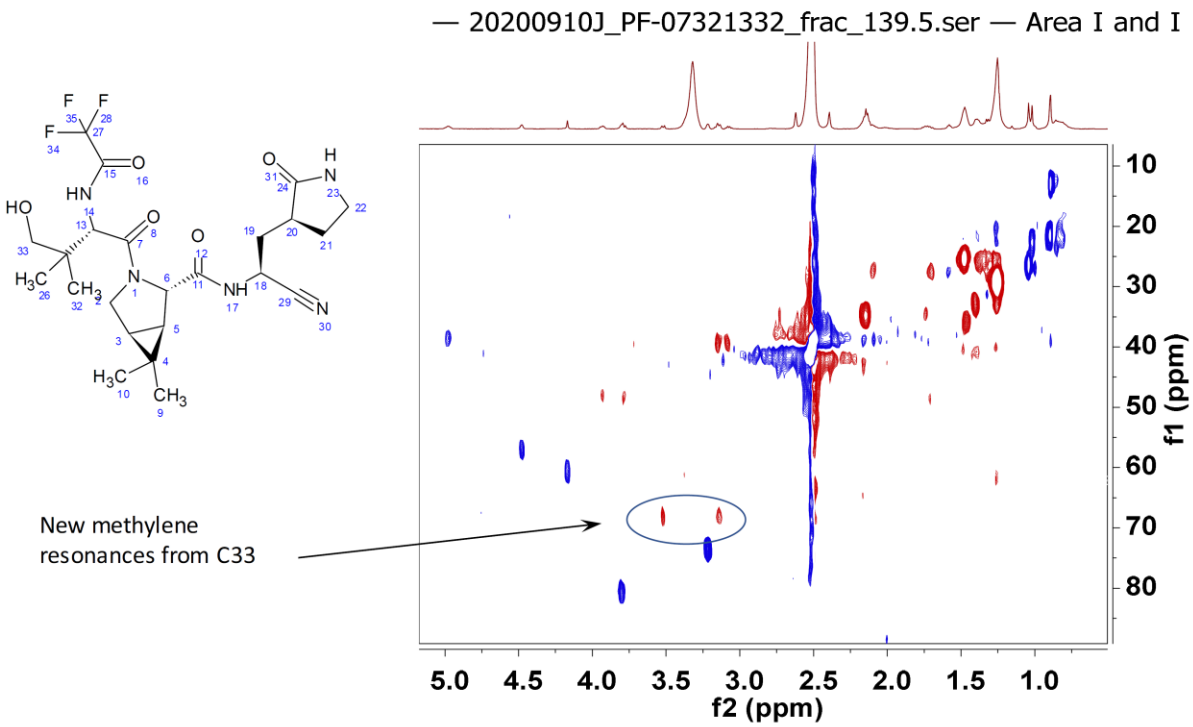

Supplemental Figure 11. High-resolution mass spectral data for metabolite M4 (PF-07329268). Top panel MS^1 spectrum; middle and lower panels are MS^2 spectra of *m/z* 498 from CID and HCD, respectively.

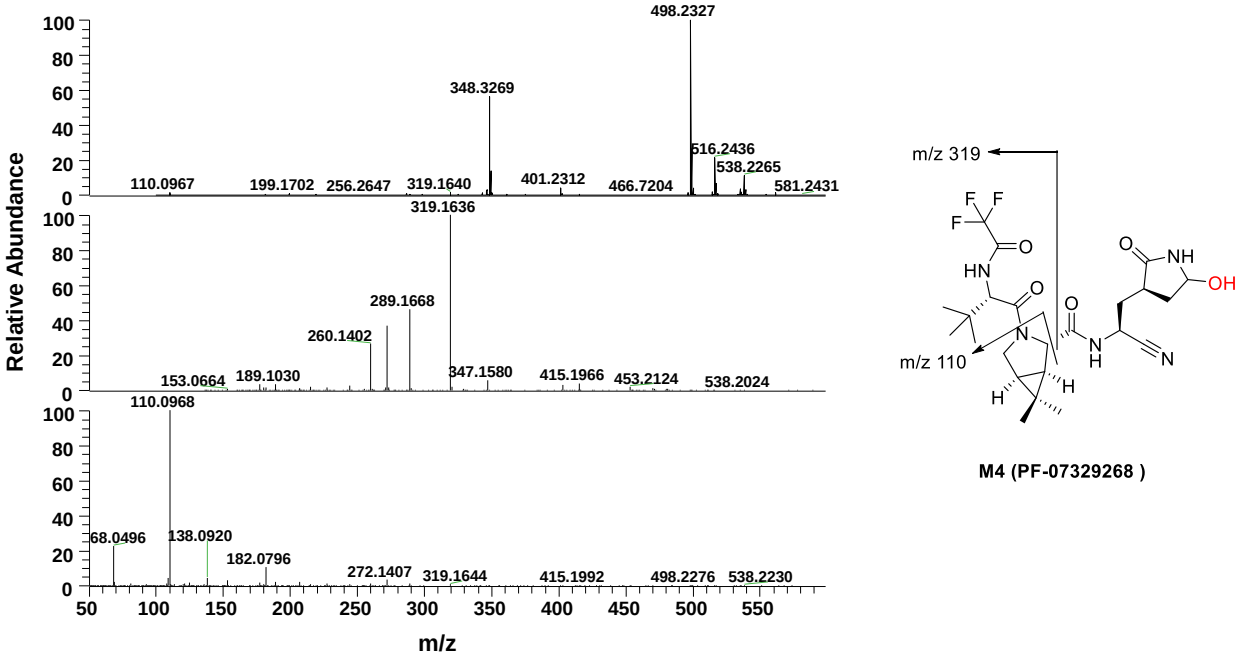

Supplemental Figure 12. ^{1}H NMR spectrum of metabolite M4 (PF-07329268).

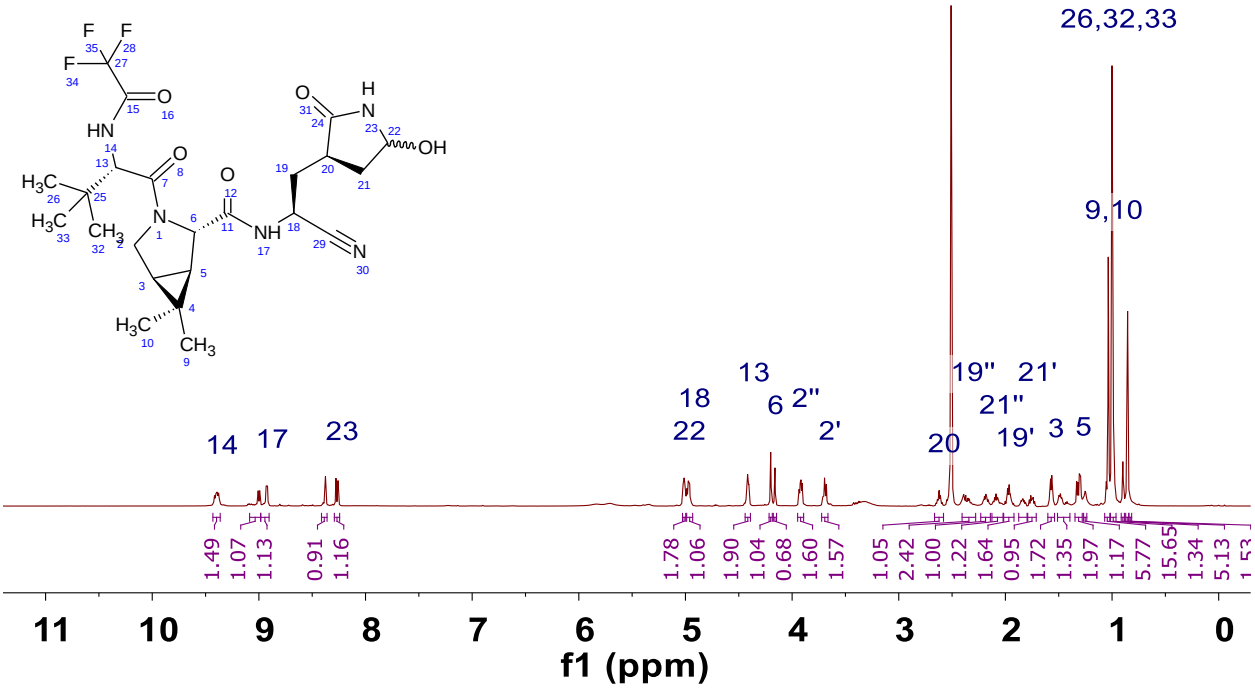

Supplemental Figure 13. 1H-13C HSQC spectral data for metabolite M4 (PF-07329268).

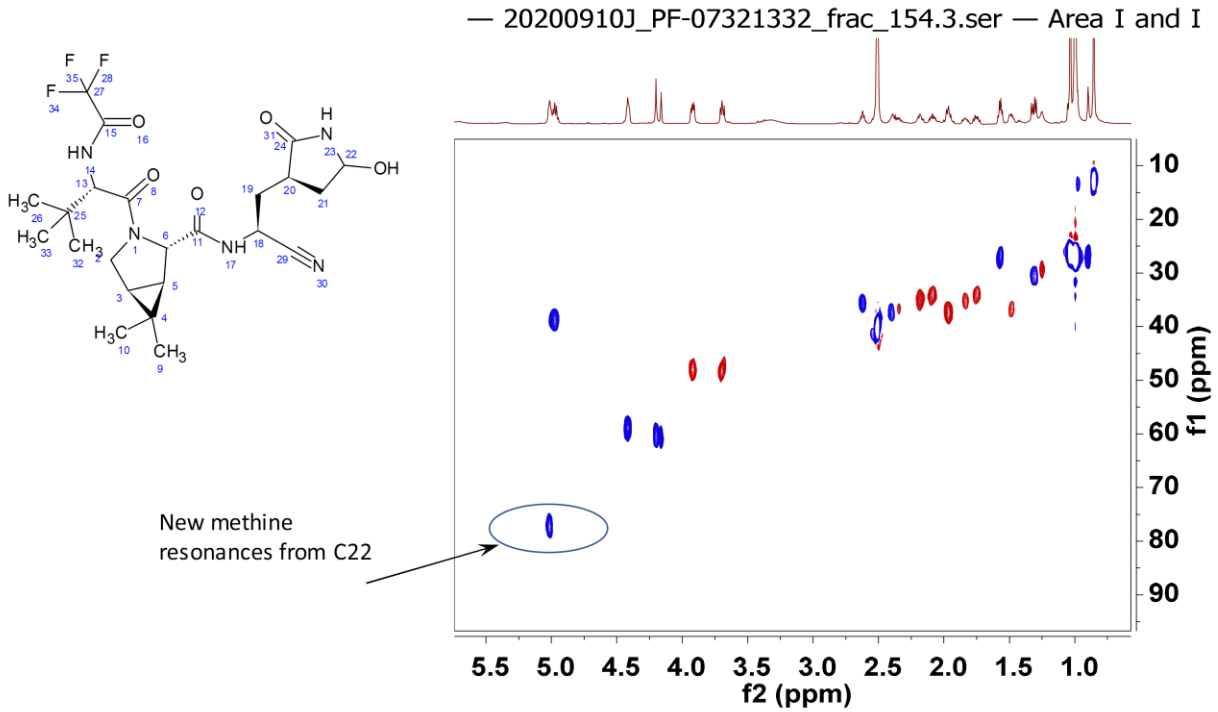

Supplemental Figure 14. High-resolution mass spectral data for dehydrogenated metabolite *m/z* 498. Top panel MS^1 spectrum; Middle and lower panels are MS^2 spectra of *m/z* 498 from CID and HCD, respectively.

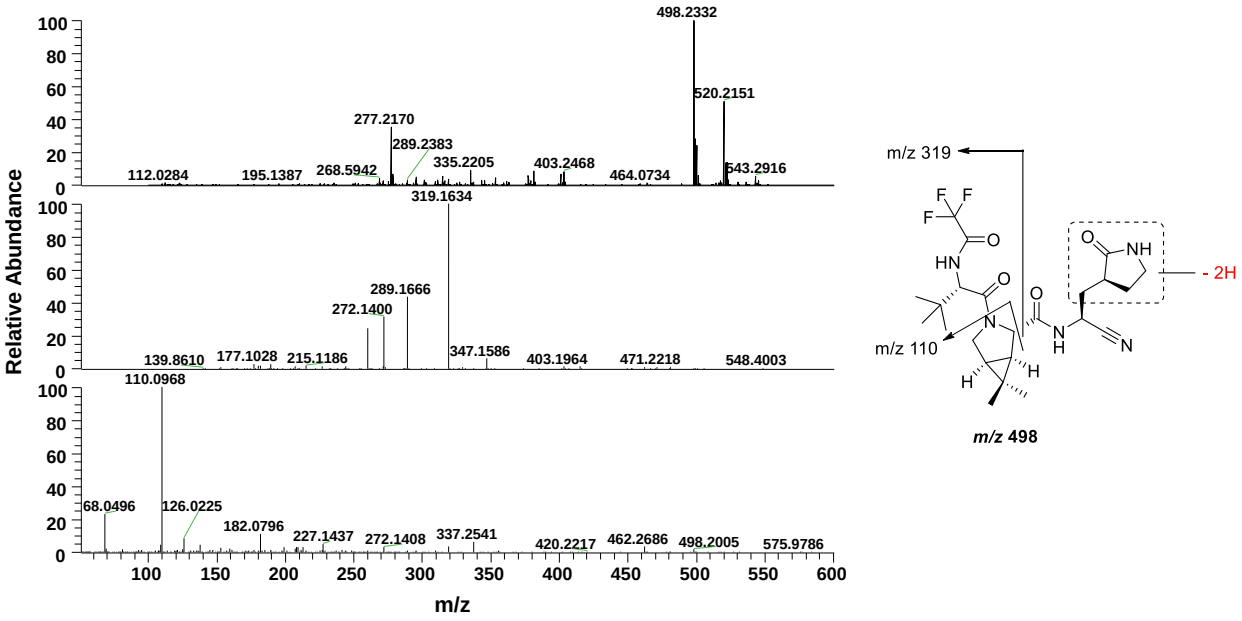

Supplemental Figure 15. Eadie-Hofstee plots for the formation of the primary PF-07321332 metabolites PF-07329265 (M1), PF-07329266 (M2), PF-07329267 (M3), and PF-07329268 (M4) following incubation of PF-07321332 (0.02–200 μM) with HLM (0.3 mg/ml).

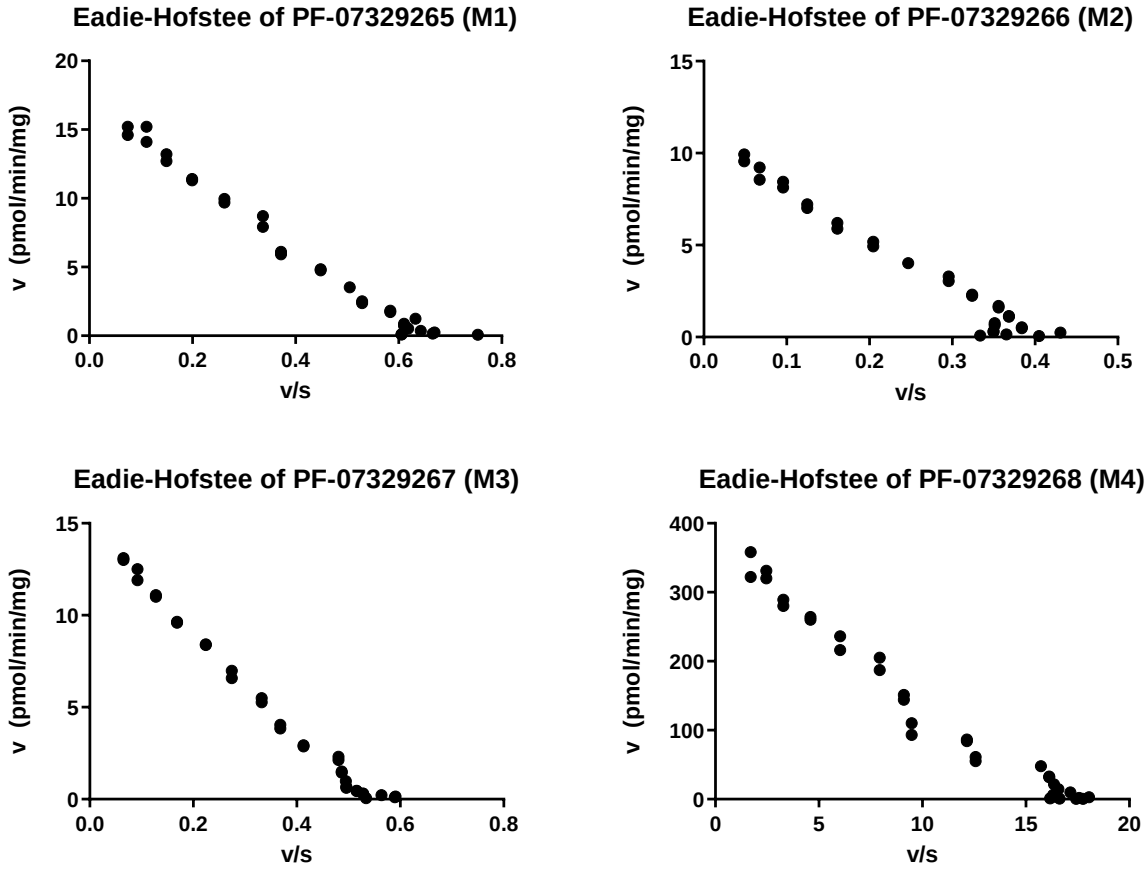

Supplemental Figure 16. IV and PO single dose PK for PF-07321332 in rats (Panel A) and monkeys (Panel B). Oral pharmacokinetics were conducted with crystalline PF-07321332 as MTBE co-solvate (rats and monkeys) and anhydrous form 1 (rats).

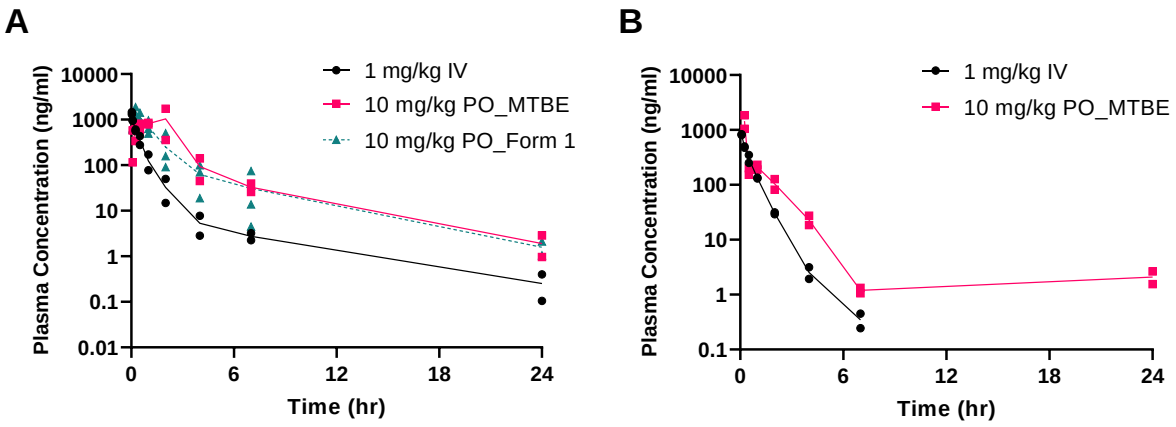

Supplementary Figure 17. Measurement of absorption spectra of CYP metabolic intermediate (MI) complexes following incubation of PF-07321332 and positive control troleandomycin with recombinant human CYP3A4, oxidoreductase, and cytochrome b5 supersomes. Spectral scans (400-500 nm) by UV-Vis spectroscopy were obtained at ~ 0, 1, 5, 10, 15, 20, 25, and 30 min.

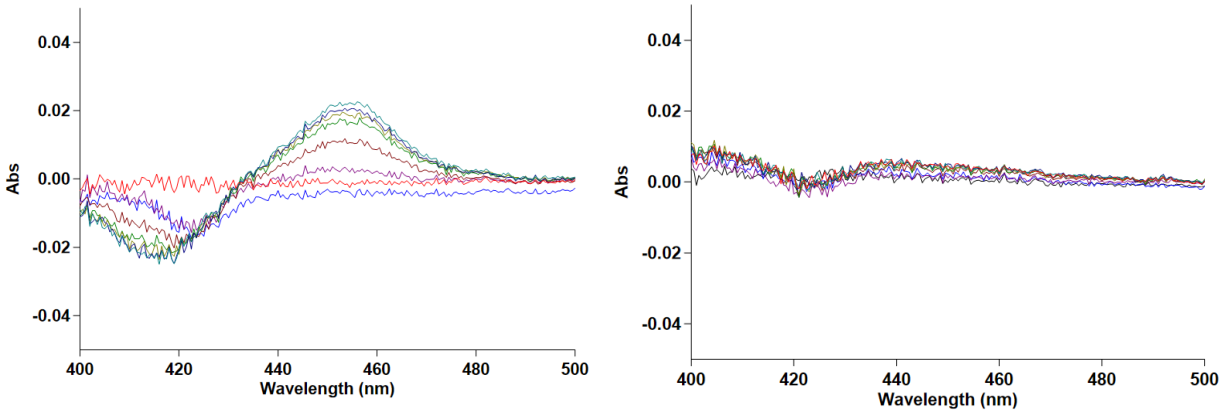

Supplemental Table 1. Permeability of PF-07321332 across caco-2 cell monolayers.

Nominal PF-07321332 Concentration (μM)	Mean A-B Permeability (SD) ($\times 10^{-6}$ cm/sec)
0.11	0.66 (0.17)
0.32	0.80 (0.15)
0.95	0.82 (0.20)
2.85	0.92 (0.16)
8.55	0.76 (0.02)
25.65	0.72 (0.08)
77.00	1.14 (0.19)
231.0	1.19 (0.13)
0.32 + 10 μM efflux inhibitor cocktail[a]	4.05 (0.26)

[a]Inhibitor cocktail = 10 μM Ko143, 10 μM PSC833, 100 μM MK571.

Supplemental Table 2. Permeability and efflux ratios of PF-07321332 in MDCKI-MDR1 and MDCKII-BCRP cells.

Compound	P_{app} AB (SD) (x 10^{-6} cm/s)	P_{app} BA (SD) (x 10^{-6} cm/s)	Efflux Ratio
MDCKI-MDR1			
PF-07321332 (0.3 μM)	0.21 (0.01)	9.94 (0.47)	48.4
PF-07321332 (0.3 μM) + PSC833 (5.0 μM)	0.75 (0.10)	1.45 (0.12)	1.9
PF-07321332 (1.0 μM)	0.12 (0.02)	10.25 (0.34)	83.7
PF-07321332 (1.0 μM) + PSC833 (5.0 μM)	0.79 (0.07)	1.34 (0.24)	1.7
PF-07321332 (3.0 μM)	0.14 (0.03)	10.03 (0.61)	71.1
PF-07321332 (3.0 μM) + PSC833 (5.0 μM)	0.62 (0.09)	1.41 (0.20)	2.3
Quinidine (0.5 μM)	1.36 (0.16)	78.22 (0.57)	57.6
Quinidine (0.5 μM) + PSC833 (5.0 μM)	21.37 (0.93)	19.77 (0.78)	0.9
MDCKII-BCRP			
PF-07321332 (0.3 μM)	1.25 (0.03)	1.82 (0.24)	1.5
PF-07321332 (1.0 μM)	1.17 (0.04)	1.81 (0.19)	1.5
PF-07321332 (3.0 μM)	1.22 (0.08)	1.77 (0.17)	1.4
Pitavastatin (0.5 μM)	0.44 (0.26)	11.08 (1.35)	24.9
Pitavastatin (0.5 μM) + Ko143 (5 μM)	4.55 (0.36)	0.87 (0.10)	0.2

Supplemental Table 3. Plasma protein binding of PF-07321332.

Species (strain)	$f_{u,p}$ [a]			
	0.3 μM	1.0 μM	3.0 μM	10 μM
Rat (Wistar-Han)	0.490	0.474	0.484	0.467
Monkey (Cynomolgus)	0.386	0.404	0.449	0.499
Human	0.296	0.300	0.311	0.333

[a]Geometric mean (*n*=12).

Supplemental Table 4. IC_{50} values for the reversible inhibition of major human cytochrome P450 (CYP) enzyme activities in HLM by PF-07321332.[a]

CYP Enzyme	Enzyme Reaction	T_0 Mean IC_{50} (95% Confidence Interval) (μM)[b]	T_{30} Mean IC_{50} (95% Confidence Interval) (μM)[c]
1A2	Phenacetin *O*-dealkylation	> 300	> 300
2B6	Bupropion hydroxylation	> 300	> 300
2C8	Amodiaquine *N*-dealkylation	> 300	> 300
2C9	Diclofenac 4'-hydroxylation	> 300	> 300
2C19	*S*-Mephenytoin 4'-hydroxylation	> 300	> 300
2D6	Dextromethorphan *O*-demethylation	> 300	> 300
3A4/5	Midazolam 1'-hydroxylation	58.3 (46.0–74.5)	27.4 (22.8–33.0)
3A4/5	Testosterone 6β-hydroxylation	106 (75.6–160)	61.1 (53.5–69.9)
3A4/5	Nifedipine oxidation	45.1 (35.4–58.0)	36.6 (29.4–45.8)

[a]Incubations with PF-07321332 (0.01–300 μM) and marker CYP substrates were conducted in NADPH (1.3 mM)-supplemented pooled HLM in the presence of $MgCl_2$ (3.3 mM) in potassium phosphate buffer (100 mM, pH 7.4). Marker CYP substrate concentrations were near enzyme affinity or Michaelis constant (K_m) values that had been previously determined and incubation times were selected based on previous determinations of reaction velocity linearity (Walsky and Obach, 2004). Incubations were conducted in duplicate and a solvent control (90/10 acetonitrile/water) was also tested. Detailed protocols including analysis of marker CYP substrate activities have been previously published (Walsky and Obach, 2004).

[b]Zero-minute preincubation (T_0) IC_{50} values.

[c]30-minute preincubation (T_{30}) IC_{50} values. A >1.5–fold shift in IC_{50} (between T_0 and T_{30}) of 2.13 (midazolam 1'-hydroxylation), 1.73 (testosterone 6β-hydroxylation), and 1.23 (nifedipine oxidation) for CYP3A4 activity was observed, which was suggestive of the potential for time-dependent inhibition (Perloff et al., 2009) of CYP3A4 by PF-07321332.

Supplemental Table 5. Kinetic Parameters for the time-, concentration-, and NADPH-dependent inhibition of CYP3A4/5 by PF-07321332 in NADPH-fortified HLM.

Probe Substrate	K_I ± SE (μM)[a]	k_{inact} ± SE (min^{-1})[b]	k_{inact}/K_I ± SE ($ml \cdot min^{-1} \cdot \mu mol^{-1}$)
Midazolam	15.5 ± 4.9	0.0142 ± 0.0013	0.916 ± 0.302
Testosterone	13.9 ± 3.0	0.0165 ± 0.0010	1.23 ± 0.29

[a] K_I = apparent inactivation concentration at half-maximal rate of inactivation. [b] k_{inact} = maximal inactivation rate. SE = standard error. Inactivation constants K_I and k_{inact} was calculated from the nonlinear regression of a three-parameter Michaelis-Menten equation using GraphPad.

Supplemental Table 6. EC_{50}, E_{max}, and γ (Hill slope) (± standard error (SE)[a]) for induction of CYP3A4 mRNA and midazolam-1'-hydroxylase activity by PF-07321332 in human hepatocytes.

	PF-07321332						
	CYP3A4 mRNA[b]			CYP3A4 Activity[b]			
Donor	EC_{50} ± SE (μM)	Ind_{max} ± SE	γ ± SE[d]	EC_{50} ± SE (μM)	Ind_{max} ± SE	γ ± SE[d]	*n*[c]
BXM	25.4 ± 2.0	30.3 ± 1.1	1.80 ± 0.22	13.2 ± 1.7	2.07 ± 0.05	2.20 ± 0.54	3
BNA	17.6 ± 1.3	33.7 ± 0.8	1.63 ± 0.15	5.82 ± 0.85	2.67 ± 0.06	1.49 ± 0.26	3
FOS	15.7 ± 10.8	18.0 ± 3.0	1.00	5.37 ± 3.53	2.19 ± 0.18	1.0	3
HH1144	30.9 ± 6.1	47.6 ± 2.9	1.00	ND[e]	ND[e]	ND[e]	3

[a]SE for PF-07321332 parameters reflects fit parameter uncertainty; Standard error (SE) for rifampin parameters determined by variability in fit parameters obtained for each independent run. [b]fold induction in CYP3A4 mRNA or enzyme activity (midazolam-1'-hydroxylase) in human hepatocytes expressed as pmol/min/10^6 cells. [c]n = number of replicates (for PF-07321332). [d]where tabulated $\gamma \neq 1.0$, CYP3A4 mRNA and activity data was fit using a four-parameter sigmoidal model; otherwise data was fit using a three-parameter sigmoidal model. [e]ND = not determined due to lack of changes (induction) in midazolam-1'-hydroxylase activity.

Supplemental Table 7. IC_{50} values for the reversible inhibition of major human intestinal, hepatobiliary, and renal transporters by PF-07321332.

Reagent System[a]	Transporter[b]	Substrate	PF-07321332 concentration (μM)	IC_{50} (μM)
HEK293 vesicles	BCRP	Rosuvastatin (0.2 μM)	0.032-1000	> 1000
HEK293 cells	MATE1	[^{14}C]-metformin (15 μM)	0.061-1000	112
HEK293 cells	MATE2K	[^{14}C]-metformin (15 μM)	0.061-1000	872
HEK293 vesicles	MDR1	*N*-methylquinidine (0.2 μM)	0.032-1000	71
HEK293 cells	OAT1	[^{3}H]-PAH (0.5 μM)	0.032-1000	> 1000
HEK293 cells	OAT3	[^{3}H]-ES (0.1 μM)	0.032-1000	521
HEK293 cells	OATP1B1	Rosuvastatin (0.3 μM)	0.032-1000	44
HEK293 cells	OATP1B3	Rosuvastatin (0.3 μM)	0.032-1000	283
HEK293 cells	OCT1	[^{14}C]-metformin (10 μM)	0.032-1000	138
HEK293 cells	OCT2	[^{14}C]-metformin (15 μM)	0.061-1000	954

[a]HEK = human embryonic kidney. Marker transporter substrate concentration used at its respective K_m for that transporter. PAH = *para*-aminohippuric acid, ES = estrone-3-sulfate

[b]BCRP = Breast cancer resistant protein, MATE = Multidrug and toxin extrusion protein, MDR = Multidrug resistance protein, OAT = Organic anion transporter, OATP = organic anion transporting polypeptide, OCT = organic cation transporter.

Supplemental Table 8. Toxicokinetic parameters for orally administered PF-07321332-MTBE co-solvate in rats and monkeys in a 2-week regulatory toxicology study.

Species	Day	Daily Oral Dose (mg/kg)	C_{max} (μg/mL)		T_{max} (h)	AUC_{24} (μg·h/mL)	
			total	unbound		total	unbound
Rat	1	60 QD	12.9 ± 1.9	6.18	0.5 ± 0.0	27.3 ± 2.4	13.1
		200 QD	37.0 ± 4.0	17.7	0.5 ± 0.0	291 ± 4	139
		1000 QD	62.1 ± 5.5	29.7	2.0 ± 1.5	796 ± 166	381
	14	60 QD	13.3 ± 5.0	6.37	0.5 ± 0.0	17.2 ± 5.1	8.24
		200 QD	27.1 ± 3.3	13.0	0.5 ± 0.0	80.5 ± 27.4	38.6
		1000 QD	51.5 ± 0.9	24.7	2.0 ± 0.0	292 ± 8	140
Monkey	1	20 BID	1.79 ± 0.89	0.779	1.3 ± 0.6	10.4 ± 5.7	4.52
		50 BID	11.3 ± 6.1	4.92	1.3 ± 1.3	84.2 ± 57.5	36.6
		300 BID	59.6 ± 11.8	25.9	3.0 ± 1.1	723 ± 152	315
	15	20 BID	2.42 ± 0.50	1.05	0.67 ± 0.26	9.61 ± 3.05	4.18
		50 BID	11.8 ± 6.6	5.13	0.92 ± 0.58	52.6 ± 28.8	22.9

300 BID	106 ± 18	46.1	3.7 ± 0.8	1220 ± 224	531